

- Pyle, A. S. Schlachter, and J. W. Stearns, Phys. Rev. Lett. **41**, 163 (1978); R. E. Olson and A. Salop, Phys. Rev. A **16**, 531 (1977).
- ⁶R. M. May, Phys. Rev. **136**, A669 (1964).
- ⁷K. Omidvar, Phys. Rev. **153**, 121 (1967).
- ⁸V. Fock, Z. Phys. **98**, 145 (1935).
- ⁹V. S. Nikolaev, Zh. Eksp. Teor. Fiz. **51**, 1263 (1966) [Sov. Phys. JETP **24**, 847 (1967)]; A. M. Halpern and J. Law, Phys. Rev. Lett. **31**, 4 (1973). These references refer to scaling which for a given multielectron target is approximately independent of the projectile charge.
- ¹⁰K. Omidvar, Phys. Rev. A **12**, 911 (1975).
- ¹¹D. P. Dewangan, J. Phys. B **8**, L119 (1975), and **10**, 1083 (1977).
- ¹²A. Tsuji and H. Narumi, J. Phys. Soc. Jpn. **41**, 357 (1976).
- ¹³R. N. Madan, Phys. Rev. A **11**, 1968 (1975).
- ¹⁴F. T. Chan and J. Eichler, to be published.
- ¹⁵J. N. Gau and J. Macek, Phys. Rev. A **10**, 522 (1974).
- ¹⁶R. E. Olson, A. Salop, R. A. Phaneuf, and F. W. Meyer, Phys. Rev. A **16**, 1867 (1977).
- ¹⁷L. I. Pivovarov, M. T. Novikov, and V. M. Tubaev, Zh. Eksp. Teor. Fiz. **42**, 1490 (1962) [Sov. Phys. JETP **15**, 1035 (1962)].
- ¹⁸P. Hvelplund, J. Heinemeier, E. Horsdal Pedersen, and F. R. Simpson, J. Phys. B **9**, 491 (1976).
- ¹⁹R. A. Phaneuf, F. W. Meyer, and R. H. McKnight, Phys. Rev. A **17**, 534 (1978).
- ²⁰H. J. Kim, R. A. Phaneuf, F. W. Meyer, and P. H. Stelson, Phys. Rev. A **17**, 854 (1978).
- ²¹K. H. Berkner, W. G. Graham, R. V. Pyle, A. S. Schlachter, and J. W. Stearns, Phys. Lett. **62A**, 407 (1977).

Melting and Staging in Graphite Intercalated with Cesium

Roy Clarke, N. Caswell, and S. A. Solin

The James Franck Institute and The Department of Physics, The University of Chicago, Chicago, Illinois 60637

(Received 6 September 1978)

The order-disorder transition in Cs-intercalated graphite has been studied using x-ray scattering. In C_8Cs the Cs layer transforms into a liquidlike phase in which the average Cs-Cs separation is incommensurate with the carbon net. Fundamentally different behavior is observed in a Cs-deficient stage-1 sample where commensurate "lattice-gas" melting occurs. Evidence is presented which shows that in low-stage material, staging is closely related to the melting transition in support of the model of Daumas and Hérold.

It is well known that certain chemical species form pure-stage graphite intercalation compounds which exhibit regular layer-stacking sequences along the c axis. In an elegant series of x-ray diffraction studies,¹ Parry and co-workers showed that whereas stage-1 C_8M ($M=K, Rb, Cs$) is three-dimensionally ordered at room temperature, n th-stage compounds $C_{12n}M$ ($n \geq 2$) contain two-dimensionally disordered M layers which order (or freeze) at $T=98, 159, \text{ and } 163$ K for $M=K, Rb, \text{ and } Cs$, respectively. More recently, Onn, Foley, and Fischer² have studied the temperature-dependent resistivity of $C_{12n}M$ ($n=2, 3$) and have observed anomalies which indicate the presence of two transitions. While stage-2 and higher-stage alkali intercalates have been extensively studied, there has been to date no quantitative analysis of the order-disorder phase transition in graphite intercalates. In addition, with the exception of a preliminary report by Ellenson *et al.*,³ melting of the M layers in stage-1 compounds has not been addressed. Moreover, the relationship between melting and staging in graphite intercalates has not been examined.

In this Letter we report x-ray-diffraction studies of stage-1 C_8Cs and of unusual stage-1-stage-2 mixtures. We will show that Cs layers in C_8Cs melt three-dimensionally and that the melting is dependent on the vapor pressure of the Cs surrounding the sample. The melting transition is either quasi second order and of the lattice-gas type, in which Cs atoms commensurately occupy preferred carbon hexagon sites, or is first order and incommensurate. To verify these points we will present data for the liquid structure factors of the melted layers. We will also discuss the applicability of the four-state Potts model⁴ to the second-order lattice-gas transition. Finally, we will show that melting and staging are closely related phenomena in graphite intercalates and we will present direct evidence in support of a model for staging which, though proposed several years ago by Daumas and Hérold,⁵ has received little attention.

Samples were prepared from highly oriented pyrolytic graphite (HOPG) using the two-bulb method of Hérold.⁶ $8 \times 8 \times 0.5$ -mm³ pieces of freshly cleaved HOPG were sealed in evacuated

Pyrex tubes (25 cm long, 8 mm i.d.) with an excess of Cs metal to provide a saturated vapor at the intercalation temperature. The samples were held at 523 K for 12 h while the Cs metal was kept at 463 K: Pure homogeneous stage-1 ordering and $\alpha\beta\gamma$ Cs-layer stacking⁷ was verified from observation of the (00 l) and (hkl) x-ray reflections, respectively. The samples were then sealed off *in situ* with a final capsule volume of about 0.5 cm³. Some of the samples were sealed off with a small excess of Cs metal to provide a saturated vapor environment. Hereafter, samples encapsulated with and without excess Cs will be referred to as "excess" and "nonexcess," respectively. The x-ray-scattering studies were carried out on a Picker automatic four-circle diffractometer with a standard 1-kW graphite-monochromated Mo $K\alpha$ source. A resistance-heated furnace was constructed which allowed the temperature of the excess Cs, if any, in the base of the sample bulb and that of the sample itself, to be varied independently. This enabled us to have some control over the vapor pressure inside the bulb. Chromel-Alumel thermocouples were placed at the base of the bulb and on the Pyrex next to the sample where the temperature stability was ± 1 K.

We consider, first, x-ray-scattering studies of excess samples. In equilibrium, it is supposed that the stoichiometry of such samples remains constant at C₈Cs in the solid phase. The structure of the Cs layer is shown in Fig. 1 with nearest-neighbor hexagon sites excluded because of the large ionic radius of Cs (1.69 Å). In the absence of a large number of vacancies, this structure cannot melt into a liquid of the lattice-gas type, commensurate with the carbon net. However, it is still possible for the filled Cs layer to melt into a liquid with an average Cs-Cs distance that is incommensurate with the carbon net and with short-range order governed primarily by the Cs-Cs interaction as in the case of a normal three-dimensional (3D) metal. Experimentally, we find that the Cs layer becomes disordered above 608 K. Figure 1(a) shows the liquidlike structure factor measured in the disordered phase of the excess sample. This is the first to be reported for an intercalate. In simple close-packed liquids, it is possible to infer the approximate nearest-neighbor distance from the position of the first peak in the liquid structure factor (LSF). Using this approach,⁹ we find that the average Cs-Cs separation in the liquid phase of the excess sample is 5.78 Å some 17% larger than in the solid phase and is close to the 5.90-Å spacing

found in the 3D Cs metal.

Because the first peak of the LSF develops at a different wave vector than the Bragg scattering we can monitor the scattering from the liquid and solid phases independently. Figure 2 shows the temperature dependence of the integrated intensity of the (100) Bragg peak (scanned between the limits, $1.389 \text{ \AA}^{-1} \leq q \leq 1.561 \text{ \AA}^{-1}$) together with an integrated section bracketing the first peak of the LSF ($1.265 \text{ \AA}^{-1} \leq q \leq 1.409 \text{ \AA}^{-1}$). The (100) Bragg peak arises solely from the (2 \times 2) lattice of the Cs layer and its integrated intensity is, therefore, a measure of the intercalate ordering. It can be seen from Fig. 2 that as the transition is approached from above, the scattering from the liquid phase decreases, and simultaneously the Bragg scattering from the solid regions grows throughout the transition range until eventually the Cs layer is completely ordered. The (100) peak remains of resolution limited width (0.02 \AA^{-1}) throughout the solid phase but in the liquid phase, the LSF grows and overlaps the position of the Bragg peak. For this reason, the integrated intensity at the position of the Bragg peak does not fall to zero above the melting point but remains at the level of the liquid scattering.

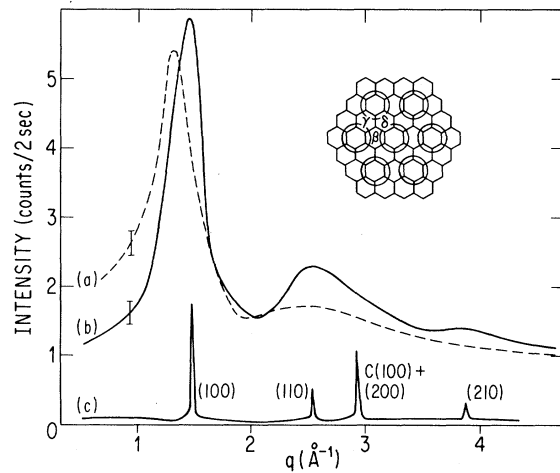


FIG. 1. Scattered-x-ray intensity (a) in disordered phase of excess sample (C₈Cs) at 700 K, (b) in disordered phase of nonexcess sample at 700 K, and (c) (hkl) reflections from C₈Cs at 300 K, indexed on the 2 \times 2 Rudorff (Ref. 8) structure shown in the inset. (Intensity scale is reduced by a factor of 10.) Step counts for 200 s were made at intervals of 0.015 \AA^{-1} for (a) and (b) and 0.005 \AA^{-1} for (c). In (a) and (b) the statistical fluctuations (vertical bars) have been averaged out and the pure-graphite (100) Bragg peak at 2.94 \AA^{-1} subtracted for clarity.

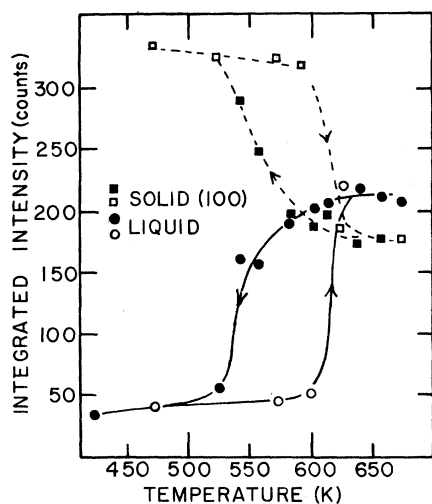


FIG. 2. Intensity of scattering from ordered phase (upper trace) and disordered phase (lower trace) of the excess sample as a function of temperature. Open symbols, heating; closed symbols, cooling. Rate of temperature change $\approx 0.2 \text{ K min}^{-1}$.

Thermal hysteresis of about 70 K is observed at the melting transition. However, the transition here is complicated by the dynamics of the intercalate in that the decrease of the packing density in the liquid phase implies that some Cs must be expelled from the sample upon melting of the Cs layer. On cooling slowly back into the ordered phase, inspection of the (00 l) and (101) reflections shows that the sample regains pure stage-1, 3D order and so Cs is replaced from the vapor during solidification. The internal strains and nucleation barrier associated with this Cs transport are probably responsible for the large amount of thermal hysteresis observed. It was possible to cycle the sample reversibly and reproducibly around the hysteresis curves shown in Fig. 2 and similar curves were obtained on a second excess sample produced under identical conditions to the first.

We now discuss experiments on nonexcess samples. The nonexcess sample, like the excess sample, was characterized as pure stage 1 after sealing the ampoule. Referring to Fig. 3, it can be seen that on the first heating cycle, the intercalate disorders at about 608 K in agreement with the behavior of the excess sample shown in Fig. 2. The (101) peak, whose behavior is shown in Fig. 3, is about ten times more intense than the (100) peak. These two reflections were found to behave identically at the transition, a clear indication that the melting is 3D. This also shows

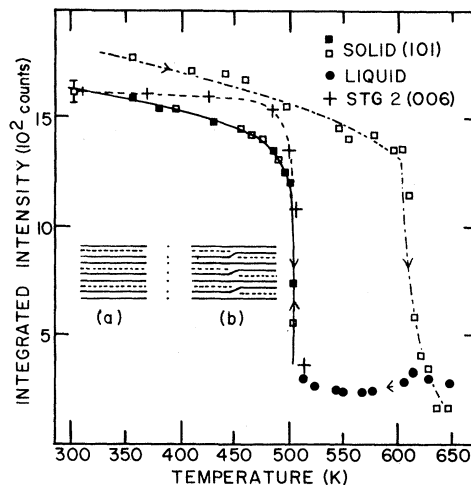


FIG. 3. Intensity of scattering from nonexcess sample as a function of temperature. The (101) peak is scanned between the limits $1.419 \text{ \AA}^{-1} \leq q \leq 1.578 \text{ \AA}^{-1}$ [intensity around the (101) peak position does not fall to zero at transition because of contributions from thermal diffuse background and liquid scattering (\bullet), centered on $q = 1.473 \text{ \AA}^{-1}$]. The solid line is the power-law fit described in the text. The stage-2 peak (+) has been normalized to the cycled (101) intensity at room temperature. Open symbols, heating; closed symbols, cooling. Inset: (a) classical stage-2 model, (b) Dumas-Hérold (Ref. 5) stage-2 model.

that order within the Cs layer and order along the c axis change simultaneously. In contrast, Ellenson *et al.*³ found from neutron-diffraction studies that C_8Rb undergoes a stacking rearrangement from $A\alpha A\beta A\gamma A\delta A$ to $A\alpha A\beta A$ prior to melting. (Here A refers to the carbon net and $\alpha, \beta, \gamma, \delta$ refer to the ordered Rb layers.) On cooling the nonexcess sample, the Bragg peak does not reappear until 503 K. Now the Cs expelled from the sample during melting does not reenter on cooling but is absorbed by the Pyrex ampoule which becomes slightly discolored. Indeed, the (00 l) reflections in the solid phase indicate that the sample is a mixture of stage 1 with 10–20% of stage 2 so that the mean layer coverage is only about 80% of its original value, as estimated from the decrease in intensity of the (101) peak in Fig. 3. On the second and subsequent heating cycles, the order-disorder transition is continuous within the resolution of the experiment (the sample temperature, which may differ slightly from the thermocouple temperature, is precise to $\pm 1 \text{ K}$).

The x-ray scattering in the disordered phase of the nonexcess sample is shown in Fig. 1(b)

and in this case the positions of the peaks in the LSF coincide with those at which Bragg scattering from the solid phase occurs, consistent with a lattice-gas disorder. We note also, the more pronounced second and third peaks in the LSF of the commensurate case relative to those in the incommensurate case reflecting the more distinct site separations in the lattice-gas model.

The four-state Potts model, of which the C_8Cs layer is an experimental realization, has been predicted to display a first-order phase transition in three dimensions,¹⁰ whereas in two dimensions a second-order transition is expected.¹¹ Accordingly, a power-law fit, $I = at^{2\beta}$, has been made to the data shown in Fig. 3, where I is the integrated intensity of the (101) reflection after the diffuse background has been subtracted, a and β are adjustable parameters, t is the reduced temperature, $t = (T_0 - T)/T_0$, and T_0 is the transition temperature. The fit was made over the range $0.004 \leq t \leq 0.40$ with $\beta = 0.046 \pm 0.01$. This value of β is significantly smaller than that expected from renormalization-group calculations for the 2D case ($\beta = 0.10$)¹² and implies that the transition is being driven weakly first order by the interlayer coupling, i.e., that the melting is 3D. Similar studies of in-plane ordering in the higher-stage intercalates with weaker interlayer coupling would, thus, be of great interest.

In Fig. 3, we have also plotted the intensity of the (006) reflection from stage-2 regions within the mixed-stage nonexcess sample just described. It is seen that the intensity of this reflection falls to background exactly at the melting point of the stage-1 regions. A full scan of the (00 l) reflections in the liquid phase reveals only stage-1 stacking. On cooling below the transition, (00 l) reflections associated with stage-2 stacking reappear. Thus, it is apparent that there is a close relationship between staging and melting in the stage-1-stage-2 mixtures. The relationship can be qualitatively understood in terms of the Dumas and Hérold (DH) model⁵ for staging which is compared with the classical model in the inset of Fig. 3. In the latter model interlayer spaces are either fully occupied or completely empty whereas all interlayer spaces contain intercalant in the DH model. Our x-ray results of Fig. 3 suggest that on melting at 608 K some cesium is expelled from each intralayer space as expected from the work of Salzano and Aronson.¹³ Subsequent cooling below 503 K results in freezing of the Cs into clusters of C_8Cs laterally contiguous to regions of stage-2 compound, the stoichiome-

try of which is unknown. The relevant x-ray line-widths indicate that the stage-1 clusters are three-dimensionally ordered with typical dimensions $>200 \text{ \AA}$. Similarly, the stage-2 regions exhibit regular c -axis stacking over distances $>200 \text{ \AA}$. On melting, cesium atoms in the C_8Cs clusters migrate to the empty interlayer spaces in the stage-2 regions thereby transforming the sample from mixed stage 1 and stage 2 to "pure" stage 1 but with a stoichiometry C_pCs with $p > 8$. Such staging via intralayer migration of intercalant atoms is the key element of the DH model. But the juxtaposition of stage-1 and -2, $\sim 200\text{-\AA}$ clusters would, in the absence of dislocations, produce unreasonably large distortions in the carbon layer planes. Thus, we suggest that low-stage intercalation compounds contain a nonnegligible number of edge dislocations.¹⁴

We gratefully acknowledge useful discussions with S. Moss, S. Nagle, and in particular P. Horn. Thanks are due J. Pluth for technical assistance and to A. W. Moore for providing the HOPG used in this study. This research was supported by the National Science Foundation Materials Research Laboratory of the University of Chicago. One of us (R.C.) acknowledges receipt of an IBM-James Franck Fellowship.

¹See, e.g., G. S. Parry, *Mater. Sci. Eng.* **31**, 99 (1977), and references therein.

²D. G. Onn, G. M. T. Foley, and J. E. Fischer, *Mater. Sci. Eng.* **31**, 271 (1977).

³W. D. Ellenson, D. Semmingsen, D. Guérard, D. G. Onn, and J. E. Fischer, *Mater. Sci. Eng.* **31**, 137 (1977).

⁴R. B. Potts, *Proc. Cambridge Philos. Soc.* **48**, 106 (1952).

⁵N. Dumas and A. Hérold, *C. R. Acad. Sci., Ser. C* **268**, 273 (1969).

⁶A. Hérold, *Bull. Soc. Chim. Fr.* **187**, 999 (1955).

⁷D. Guérard, P. Langrange, M. El Makrini, and A. Hérold, to be published.

⁸W. Rudorff and E. Schulze, *Z. Anorg. Chem.* **277**, 156 (1954).

⁹H. P. Klug and L. E. Alexander, *X-ray Diffraction Procedures for Polycrystalline and Amorphous Materials* (Wiley, New York, 1974).

¹⁰R. G. Priest and T. C. Lubensky, *Phys. Rev. B* **13**, 4159 (1976).

¹¹E. Domany, M. Schick, and J. S. Walker, *Phys. Rev. Lett.* **38**, 1148 (1977).

¹²A. N. Berker, S. Ostlund, and F. A. Putnam, *Phys. Rev. B* **17**, 3650 (1978).

¹³F. J. Salzano and S. Aronson, *J. Chem. Phys.* **42**, 1323 (1965).

¹⁴P. Guyot and J. M. Gjurasevic, *Rev. Phys. Appl.* **11**, 356 (1976).